ISOTROPIC 3D SILICON HALL SENSOR

Christian Sander, Carsten Leube, Taimur Aftab, Patrick Ruther and Oliver Paul
Department of Microsystems Engineering (IMTEK), University of Freiburg, Germany

ABSTRACT

This paper reports the first three-dimensional (3D) Hall sensor with isotropic sensitivity for the three spatial components of the magnetic field. The silicon device has the shape of a hexagonal prism with symmetric sets of three contacts on its top and bottom surfaces. Sending currents obliquely across the device allows one to operate it as three mutually crossing, identical, and effectively orthogonal Hall sensors. The sensitivity vectors of these Hall sensors are easily converted into sensitivities in the Cartesian coordinate system *xyz*. We demonstrate a design achieving sensitivities of S_x = 33.0 mV/VT, S_y = 33.9 mV/VT and S_z = 33.3 mV/VT.

INTRODUCTION

Magnetic field sensors based on the Hall-effect in silicon (Si) are nowadays most widely used for contactless position measurements. Traditional planar Hall-effect transducers are sensitive to only one component of the magnetic flux density $\boldsymbol{B}$. For the purpose of measuring all three spatial components (B_x, B_y, and B_z) of $\boldsymbol{B}$, three separate, orthogonally aligned devices have been used, as illustrated in figure 1(a). Drawbacks of this approach are the costly assembly, the challenging orthogonal alignment during assembly, the spatial resolution limit due to the distance among sensor chips, and the handling of 12 contacts [1]. An alternative concept is to co-integrate a planar Hall plate with two vertical Hall sensors (VHS) [2,3]. However, the vertical Hall structures show lower sensitivities and higher offsets and thus require separate signal conditioning circuitry for compensation [4,5]. Furthermore, the number of contacts remains an issue. Integrated devices using only one active region may have fewer contacts and potentially offer increased spatial resolution. However, the lack of a fourfold symmetry, the inherently different sensitivities of the individual channels and cross-sensitivities between channels lower the overall performance [6,7]. No semiconductor magnetic field sensor is currently able to measure three orthogonal components of $\boldsymbol{B}$ with equal sensitivities and similar offsets.

In this paper we present the first 3D Hall device fulfilling these requirements. Section 2 introduces the novel sensor concept. The fabrication process is illustrated in Section 3, following with the experimental results in Section 4.

SENSOR DESIGN

The ideal planar Hall-effect device is a rotational symmetric plate with four peripheral contacts. Its output voltage can be written as

$$V_{\mathrm{out}}(B) = V_{\mathrm{Hall}}(B) + V_{\mathrm{off}} = SV_{\mathrm{in}}B + V_{\mathrm{off}} \qquad (1)$$

where B, $S = V_{\mathrm{in}}^{-1}\partial V_{\mathrm{out}}/\partial B$, V_{Hall}, V_{in}, and $V_{\mathrm{off}} = V_{\mathrm{out}}(B = 0)$ denote the out-of-plane magnetic flux density, the voltage-related sensitivity, the Hall voltage, the drive voltage and the offset of the device in the absence of a magnetic field, respectively. Usually, V_{Hall} is obtained by the spinning-current method, where the biasing and sensing contacts are cyclically permuted four times and the output voltage is averaged, thus effectively eliminating V_{off} [8].

With properly dimensioned contacts, one achieves maximum S with a value of $0.47\mu_{\mathrm{H}}$ [9,10], where μ_{H} denotes the Hall mobility. One such optimal sensor geometry is a square shaped device with four identical contacts centered on its four sides. This suggests that an ideal 3D magnetic field sensor with isotropic sensitivities could be a conductive cube with one contact centered on each of its six faces as shown in Fig. 2(a). The sensor can be operated as three equivalent, orthogonal Hall plates in three orthogonal planes defined by three groups of four contacts. The corresponding sensitivity vectors $\boldsymbol{S}_{x'} = (S_{x'},0,0)$, $\boldsymbol{S}_{y'} = (0,S_{y'},0)$, and $\boldsymbol{S}_{z'} = (0,0,S_{z'})$ are mutually orthogonal, have identical magnitude, and allow the measurement of the components of $\boldsymbol{B}$, i.e., $B_{x'}$, $B_{y'}$, and $B_{z'}$. Since deep buried contacts cannot be realized in standard IC technology, we deformed the cube so that its contacts are relocated to the top and bottom surfaces of a wafer. This deformation is illustrated in figures 2(b) and (c). Contacts 1, 3, and 5 adjacent to one corner of the cube thereby move to the top surface, while contacts 2, 4, and 6 adjacent to the diagonally opposite corner are relocated to the bottom surface. The diagonal axis connecting these corners becomes an axis perpendicular to the wafer. As a result, the cube is deformed into a hexagonal prism and the sensor is symmetric under 120° rotation in the *xy* plane. Again, the device can be operated in three planes, as indicated in

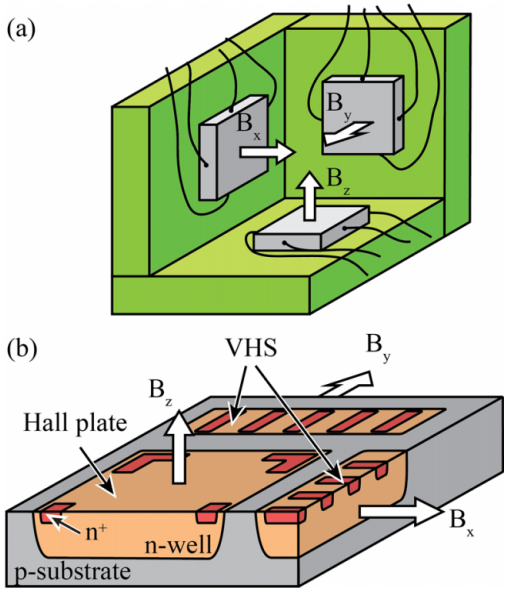

Figure 1: (a) Classic implementation of a three-axis magnetic field sensor consisting of three orthogonal Hall plates and (b) schematic of an integrated three-axis magnetic field sensor using a Hall plate und two orthogonal VHS.

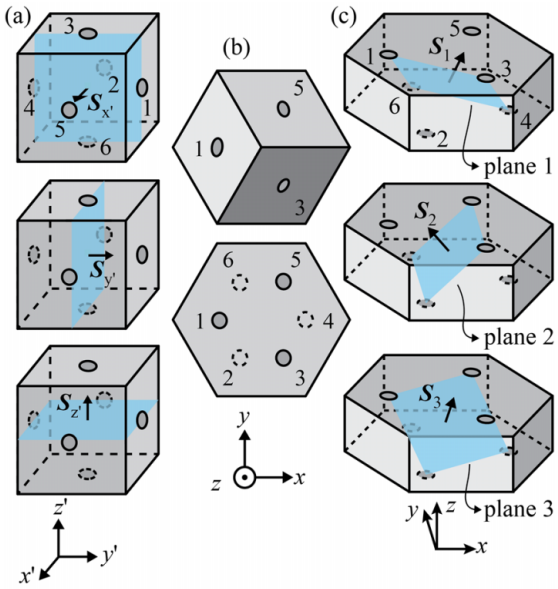

Figure 2: Schematic of (a) an ideal 3D Hall cube with all three operation planes and respective sensitivity vectors $\boldsymbol{S}_{x'}$, $\boldsymbol{S}_{y'}$ and $\boldsymbol{S}_{z'}$, (b) a diagonal view of the cube and its projection onto two parallel xy-planes and (c) the novel hexagonal 3D Hall device with its three operation planes and respective sensitivity vectors $\boldsymbol{S}_1$, $\boldsymbol{S}_2$ and $\boldsymbol{S}_3$.

figure 2(c). For a properly dimensioned device, the sensitivity vectors $\boldsymbol{S}_1 = (S_{1x}, S_{1y}, S_{1z})$, $\boldsymbol{S}_2 = (S_{2x}, S_{2y}, S_{2z})$, $\boldsymbol{S}_3 = (S_{3x}, S_{3y}, S_{3z})$ corresponding to these three planes are again orthogonal; using $S_{ij} = (\partial V_{\mathrm{Hall},i}/\partial B_j)/V_{\mathrm{in}}$, with planes i = 1,2,3 and directions j = x,y,z. In view of the device symmetry they have the same magnitude S_0. In the *xyz* coordinate system the normalized sensitivity vectors have the components listed in Table 1. These coefficients are the direction cosines of the sensitivity vectors with respect to the x, y, and z axes. They constitute the ideal orthogonal transformation matrix $\boldsymbol{O}$ mapping the normal base vectors of the *xyz* coordinate system onto those defined by the normalized sensitivities.

FABRICATION AND ASSEMBLY

Figure 3 shows a micrograph of a 3D Hall-effect sensor fabricated according to this novel concept, a schematic defining the relevant geometrical parameters listed in Table 2, and a photograph of a printed circuit board (PCB) -mounted device ready for characterization. The fabrication process is summarized in figure 4. It combines insulation, contact diffusion, metallization, and dual-side deep reactive ion etching (DRIE). A patterned thermal oxide layer (700 nm) on the front and rear of an n-doped Si wafer {Fig. 4(a)} serves as an implantation mask for

Table 1: Normalized values of the sensitivity matrix $\boldsymbol{O}$ for the ideal hexagonal 3D Hall sensor.

normalized sensitivity components	sensitivity direction j			
	x	y	z	
S_{1j}/S_0	0.408	0.707	0.577	} = $\boldsymbol{O}$
S_{2j}/S_0	−0.816	0	0.577	
S_{3j}/S_0	0.408	−0.707	0.577	

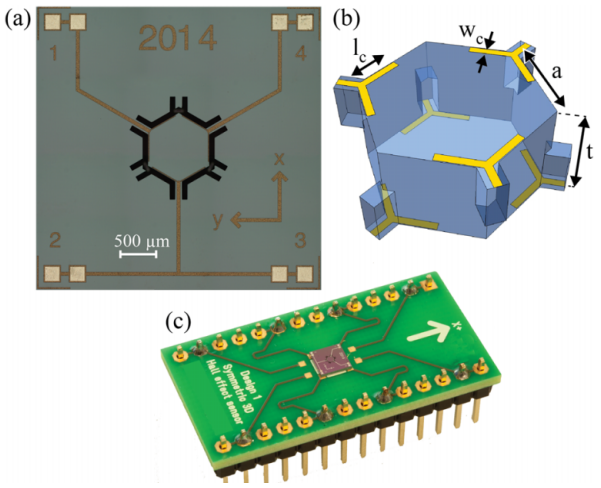

Figure 3: (a) Micrograph of the novel sensor, (b) schematic with relevant geometry parameters and (c) assembled device.

Table 2: Geometry parameters of the device.

Parameter	t	a	l_c	w_c
(µm)	525	492	442	10

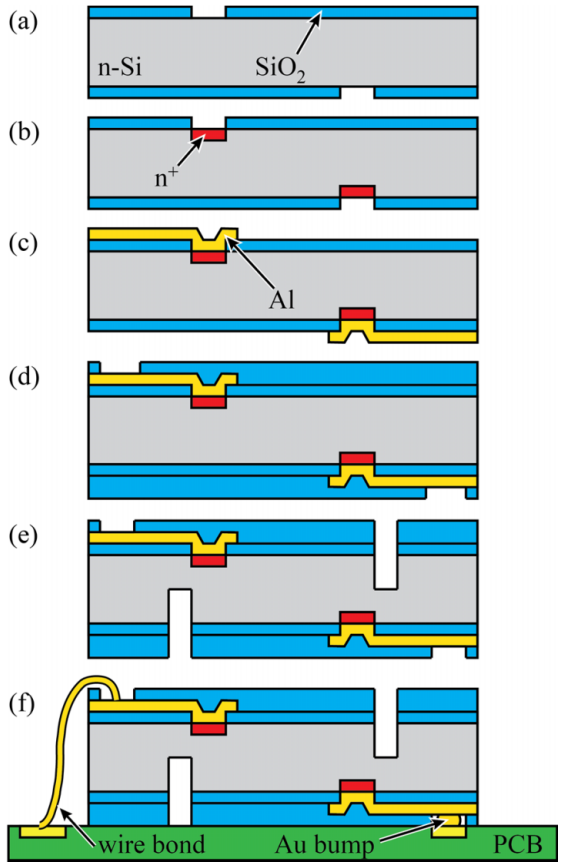

Figure 4: Fabrication process and assembly of the 3D Hall sensor including (a) insulation, (b) ion implantation, (c) metalization, (d) passivation, (e) DRIE, and (f) flip-chip and wire-bonding.

n^+ contacts {Fig. 4(b)}. The implantation energy is 80 keV with a dose of 2×10^{16} cm^{-2} for phosphorus ions. An Al metallization (500 nm) is then sputtered on the front and rear and patterned using wet etching {Fig. 4(c)}.

Subsequently, a low temperature oxide (LTO) passivation (2 µm) is deposited and structured using reactive ion etching (RIE) to expose the contact pads {Fig. 4(d)}. The hexagonal shape is defined by DRIE to the depth of 270 µm from both sides {Fig. 4(e)}. As a result of the mask design, the prism is suspended by six bridges with a height and width of about 255 µm and 100 µm, respectively. The rear electrical interconnection is performed by flip-chip bonding the sensor chip onto a PCB, whereas the front contacts are wire-bonded to it {Fig. 4(f)}.

EXPERIMENTAL RESULTS

The electrical characterization of the novel device was performed using the parameter analyzer 4156C from Agilent. A 3D Helmholtz coil setup served to extract the electric field dependent sensitivities of the devices up to 3.6 mT.

As mentioned, the device can be operated in three planes defined by three groups of four contacts. The offset characteristic for one plane is shown in figure 5. For each plane the measurement is performed in four modes applying the spinning-current method [8]. The single-mode offset V_{off} increases linearly with the input voltage V_{in}. For all modes $|V_{off}|$ is about 1% of V_{in}. The residual offset V_{res} of about 6.3 µV at $V_{in} = 1$ V obtained by averaging over the four modes is smaller than $|V_{off}|$ by a factor of more than 1500. The input resistances R_{in} for Modes 1 and 3, and Modes 2 and 4 are 259.3 Ω and 262.5 Ω, respectively. The deviation is likely due to fabrication imperfections.

The Hall response $\boldsymbol{V}_{Hall} = (V_{Hall,1}, V_{Hall,2}, V_{Hall,3})$ after current spinning for all three operation planes ($i = 1,2,3$) at $V_{in} = 1$ V is shown in figure 6. For each plane, three sensitivity values using again $S_{ij} = (\partial V_{Hall,i}/\partial B_j)/V_{in}$, with $j = x, y$, and z, are extracted. They constitute the sensitivity matrix $\boldsymbol{T}_{meas}$ listed in Table 3 together with the normalized values forming the measured transformation matrix $\boldsymbol{O}_{meas}$. The elements of $\boldsymbol{O}_{meas}$ are again the direction cosines of the sensitivity vectors, now experimentally determined, with respect to the x, y, and z coordinate axes. These values are in good agreement with those of $\boldsymbol{O}$ in Table 1. This reflects the fact that the directions of the measured sensitivity vectors $\boldsymbol{S}_1$ to $\boldsymbol{S}_3$ are close to those of the ideal device in figure 1(c). To evaluate the sensitivities and angular error with respect to the xyz coordinate system, the measured sensitivity vectors $\boldsymbol{S}_1$ to $\boldsymbol{S}_3$ are transformed using the ideal

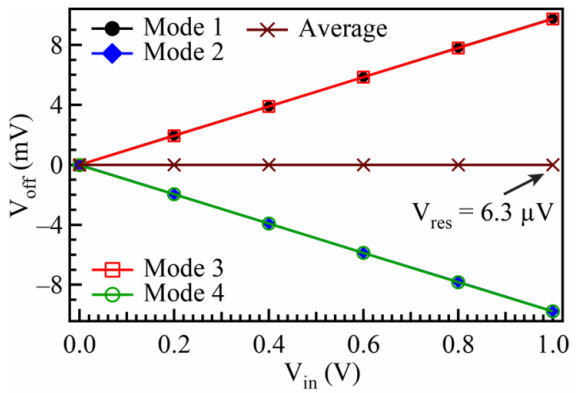

Figure 5: Offset voltage V_{off} and residual offset V_{res} after current-spinning as a function of the input voltage V_{in} for a representative plane.

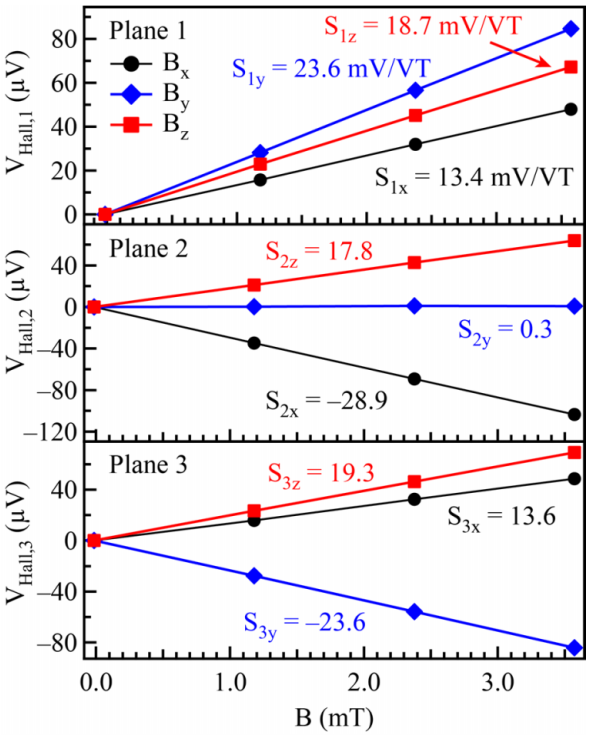

Figure 6: Hall voltage $V_{Hall,i}$ for each plane ($i = 1,2,3$) as a function of the spatial components of the magnetic field B_j ($j = x,y,z$), including the extracted sensitivities $S_{ij} = (\partial V_{Hall,i}/\partial B_j)/V_{in}$.

Table 3: Measured and normalized values of the sensitivities for the realized hexagonal 3D Hall sensor.

sensitivity components	sensitivity direction j x	y	z	
S_{1j} (mV/VT)	13.4	23.6	18.7	$= \boldsymbol{T}_{meas}$
S_{2j} (mV/VT)	−28.9	0.3	17.8	
S_{3j} (mV/VT)	13.6	−23.6	19.3	
normalized values				
$S_{1j}/\lvert\boldsymbol{S}_1\rvert$	0.406	0.716	0.568	$= \boldsymbol{O}_{meas}$
$S_{2j}/\lvert\boldsymbol{S}_2\rvert$	−0.851	0.008	0.525	
$S_{3j}/\lvert\boldsymbol{S}_3\rvert$	0.408	−0.706	0.579	

transformation matrix $\boldsymbol{O}$. The transformed sensitivities are calculated as $\boldsymbol{S}_x = (33.0,-0.1,-0.4)$ mV/VT, $\boldsymbol{S}_y = (-1.3,33.9,-1.7)$ mV/VT and $\boldsymbol{S}_z = (0,0,33.3)$ mV/VT, respectively. The angular errors between these sensitivity vectors and the corresponding axes of the xyz coordinate system are found to be $\Delta x = 0.7°$, $\Delta y = 3.6°$ and $\Delta z = 0.1°$, showing the already high degree of isotropy and orthogonality of this initial device.

In practice, the three components of the magnetic field are accurately calculated by multiplying the inverse of the measured sensitivity matrix $\boldsymbol{T}_{meas}$ with the vector of the three Hall voltages after current spinning $\boldsymbol{V}_{Hall}$. For illustration we applied a reference field vector $\boldsymbol{B}$ with a magnitude of 3.5 mT and rotated it in the xy, xz and yz plane from 0° to 90° in steps of 5°. At each step we extracted the measured field vector by $\boldsymbol{B}_{meas} = \boldsymbol{T}_{meas}^{-1} \boldsymbol{V}_{Hall}$. The result is shown in figure 7. The overall deviation of the measured $\boldsymbol{B}$-field magnitude from the nominal value of 3.5 mT is only 0.1±0.9%. The extracted $\boldsymbol{B}$ vectors show an angular

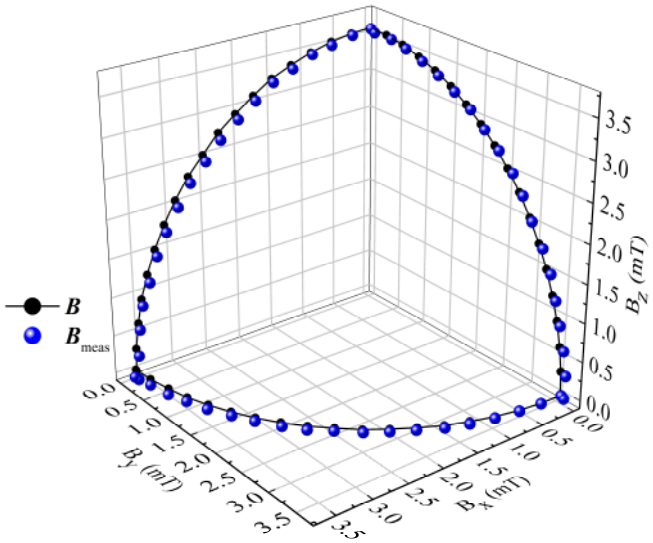

Figure 7: Measured magnetic field vector $\boldsymbol{B}_{meas}$ *for an applied reference field* $\boldsymbol{B}$.

deviation from the direction of the applied $\boldsymbol{B}$ field of 0.8±0.4°.

CONCLUSION

The novel 3D Hall-effect sensor shows a highly isotropic response to the magnetic field. In view of its symmetry, it can be operated with the same drive and compensation circuitry for its three sensitive planes. It has to be noted that the current device is a discrete component lending itself for hybrid integration with drive and signal conditioning circuitry. This can possibly be achieved by multi chip stacking assembly. Co-integration with on-chip circuitry will likely require additional technological developments, since the low doping of the substrate used for the sensor is not the standard doping of CMOS substrates.

REFERENCES

[1] E. Ramsden, *Hall Effect Sensors – Theory and Applications*, 2nd ed., Elsevier, Netherlands, 2006.

[2] F. Burger, P-A. Besse, and R. S. Popovic, "New fully integrated 3-D silicon Hall sensor for precise angular-position measurements", *Sensors and Actuators A: Physical*, vol. 67, pp. 72-76, 1998.

[3] P. Kejik, E. Schurig, F. Bergsma, R.S. Popovic, "First fully CMOS-integrated 3D Hall probe", in *Digest Tech. Papers Transducers'05 Conference*, Seoul, 2005, pp. 317-320.

[4] J. Pascal, L. Hébrard, V. Frick, J.-B. Kammerer, J.-P. Blondé, "Intrinsic limits of the sensitivity of CMOS integrated vertical Hall devices", *Sensors and Actuators A: Physical*, vol. 152, pp. 21-28, 2009.

[5] O. Paul, R. Raz, T. Kaufmann, "Analysis of the offset of semiconductor vertical Hall devices", *Sensors and Actuators A: Physical*, vol. 174, 2012.

[6] Ch. Roumenin, K. Dimitrov, A. Ivanov, "Integrated vector sensor and magnetic compass using a novel 3D Hall structure", *Sensors and Actuators A: Physical*, vol. 92, pp 119-122, 2001.

[7] S. Lozanova, Sv. Noykov, Ch. Roumenin, "A novel 3-D Hall magnetometer using subsequent measurement method", *Sensors and Actuators A: Physical*, vol. 153, pp. 205-211, 2009.

[8] P. Munter, "A low-offset spinning-current Hall plate", *Sensors and Actuators A: Physical*, vol 22, pp. 743-746, 1989.

[9] R.S. Popovic, *Hall Effect Devices*, 2nd ed., The Adam Hilger Series on Sensors, IOP Publishing Ltd., Bristol, 1991.

[10] O. Paul, M. Cornils. "Explicit connection between sample geometry and Hall response", *Appl. Phys. Lett.*, vol. 95, 232112, 2009.

CONTACT

C. Sander, tel: +49-761-2037193;
christian.sander@imtek.de